

https://doi.org/10.1070/QEL16654

On the thermal noise limit of ultrastable optical cavities

N.O. Zhadnov, K.S. Kudeyarov, D.S. Kryuchkov,
I.A. Semerikov, K.Yu. Khabarova, N.N. Kolachevsky

Abstract. **We consider two methods of lowering thermal noise, which limits the attainable frequency stability of lasers stabilised to a high-Q external Fabry–Perot cavity. These are cavity lengthening and use of high-Q mechanical materials in the production of its constituent parts. The results of numerical simulation are outlined for the horizontal and vertical suspension systems of the cavity body and its sensitivity to vibrations in these cases. The progress in the development of ultrastable laser systems using cryogenic silicon cavities is also discussed.**

Keywords: *ultrastable cavities, thermal noise, vibrational sensitivity of cavities.*

1. Introduction

The development of laser sources with a spectral linewidth less than 1 Hz is a major avenue in the modern physics of high-precision measurements. Initially aimed at solving the tasks of precision spectroscopy, this research largely paved the way to the progress in the area of frequency standards and lent impetus to the development of new areas, such as gravitational wave detection [1], studies of interparticle interactions in quantum gases [2], and the development of femtosecond optical frequency combs [3]. Ultrastable lasers are employed for the spectroscopy of ultranarrow clock transitions in optical frequency standards based on atomic ensembles [4] and single atoms [5]. On a shorter averaging time than the time of particle ensemble preparation and measurement, the optical clock stability is completely determined by the frequency stability of laser radiation. On a longer time, the clock stability may be limited by the Dick effect [6], which is also determined by the level of laser noise. For a frequency instability of laser radiation of $\sim 10^{-15}$, the contribution made by the Dick effect may far exceed the fundamental limit imposed by quantum noise [7]. That is why the further progress of optical frequency standards aimed at attaining precision and stability at a level of 10^{-18} and better calls for a more efficient stabilisation of laser radiation frequency [8].

The key element of an ultrastable laser system is a passive monolithic high-Q Fabry–Perot cavity with an as high as possible stability of the mirror separation. The frequency of the laser light is stabilised to the cavity transmittance peak with the use of a feedback loop. The most frequently used method of frequency stabilisation to external cavity mode is the phase-modulation Pound–Drever–Hall technique [9], which has proved itself to be advantageous. To date, the best fractional instability of the laser frequency over an averaging time of 1–100 s amounts to $\sim 10^{-17}$, which was obtained using a silicon cryogenic cavity [10] and a ULE-glass cavity of length ~ 0.5 m [11].

In this work we consider the use of such cavities in ultrastable laser systems. In Sections 2 and 3 we discuss the thermal noise limit, which limits the cavity stability, and the methods for lowering this fundamental limit. The latest results in the development of ultrastable lasers for an optical frequency standard based on strontium atoms are outlined in Sections 4 and 5.

2. Thermal noise and cavity stability

The stability of the frequency ν of Fabry–Perot cavity eigenmodes is determined primarily by the stability of its mirror separation $\hat{L}$:

$$\frac{\Delta\nu}{\nu} = -\frac{\Delta\hat{L}}{\hat{L}}, \tag{1}$$

The relative displacement of the cavity mirrors may result from the fluctuations of the cavity body length due to temperature variations or vibrations, but their effect may be effectively suppressed by isolating the cavity from external perturbation factors. The fundamental limitation on the stability of mirror separation is imposed by the thermal motion of interferometer body particles (thermal noise).

In formula (1), $\hat{L}$ is not the absolute distance between the geometric centres of two mirrors, which is impossible to stabilise with an accuracy of 10^{-15}, but the generalised coordinate, which characterises the cavity length. It may be shown [12] that the phase shift of a laser beam with a radiation intensity profile $g(\boldsymbol{r})$ in its reflection from the mirror surface distorted by thermal vibrations is expressed as

$$\Delta\phi(t) = \int_S g(\boldsymbol{r})\boldsymbol{k}\boldsymbol{u}(\boldsymbol{r},t)\,\mathrm{d}^2 r, \tag{2}$$

N.O. Zhadnov, K.S. Kudeyarov, D.S. Kryuchkov, I.A. Semerikov, K.Yu. Khabarova P.N. Lebedev Physical Institute, Russian Academy of Sciences, Leninsky prosp. 53, 119991 Moscow, Russia; e-mail: kseniakhabarova@gmail.com;
N.N. Kolachevsky P.N. Lebedev Physical Institute, Russian Academy of Sciences, Leninsky prosp. 53, 119991 Moscow, Russia; All-Russia Research Institute of Physical and Radio Engineering Measurements (VNIIFTRI), 141570 Mendeleevo, Moscow region, Russia; Russian Quantum Centre, ul. Novaya 100, Skolkovo, 143025 Moscow, Russia

Received 21 February 2018; revision received 16 March 2018
Kvantovaya Elektronika **48** (5) 425–430 (2018)
Translated by E.N. Ragozin

Here, the integral is taken over the mirror surface S; $\boldsymbol{r}$ is the position vector of a point on the mirror surface; $\boldsymbol{u}(\boldsymbol{r},t)$ is the displacement of the mirror point with coordinate $\boldsymbol{r}$ from its unperturbed position; $\boldsymbol{k}$ is the wave vector of the incident radiation aligned with the z axis, which is perpendicular to the mirror surface. By using the phase shift $\Delta\phi(t)$, it is possible to introduce the effective surface displacement along the z axis for one of the mirrors:

$$U_z(t) = \frac{\Delta\phi(t)}{|\boldsymbol{k}|} = \int_S g(\boldsymbol{r}) u_z(\boldsymbol{r},t)\,\mathrm{d}^2 r. \tag{3}$$

Although the cavity mirror is a complex object with a multitude of degrees of freedom, its effect on the phase of laser radiation may be characterised by one generalised coordinate (3). The power spectral density of the thermal fluctuations of the quantity $U_z(t)$ may be calculated using the fluctuation-dissipative theorem and the approach introduced in Ref. [13]. The formulas for the power spectral density of the thermal noise of the mirrors, G_m, and the cavity body, G_sp, are given in Ref. [14]:

$$G_\mathrm{m}(f) = \frac{4k_\mathrm{B}T}{2\pi f}\frac{1-\sigma_\mathrm{sub}^2}{\sqrt{\pi}E_\mathrm{sub}w_0}\frac{1}{Q_\mathrm{sub}} \times\left(1+\frac{2}{\sqrt{\pi}}\frac{1-2\sigma_\mathrm{sub}}{1-\sigma_\mathrm{sub}}\frac{Q_\mathrm{sub}}{Q_\mathrm{coat}}\frac{D}{w_0}\right), \tag{4}$$

$$G_\mathrm{sp}(f) = \frac{4k_\mathrm{B}T}{2\pi f}\frac{L}{3\pi R^2 E_\mathrm{sp}}\frac{1}{Q_\mathrm{sp}}, \tag{5}$$

where E is the Young modulus; Q is the mechanical Q-factor; σ is the Poisson coefficient; subscripts sp, sub, and coat apply to the materials of the cavity body, the mirror substrates, and the reflective coating, respectively; f is the frequency; k_B is the Boltzmann constant; T is the temperature; D is the thickness of the reflective coating; w_0 is the radius of the radiation beam on the mirror; and L and R are the length and radius of the cavity body. The fractional mode frequency instability may be calculated from the total spectral noise power $G_\mathrm{tot}(f) = 2G_\mathrm{m}(f) + G_\mathrm{sp}(f)$ using the formula [15]

$$\sigma_y = \frac{\sqrt{2\ln 2}\sqrt{fG_\mathrm{tot}(f)}}{L}. \tag{6}$$

The working temperature of the cavity is selected at its 'zero CTE point', i.e. the temperature at which the thermal expansion coefficient of the material is equal to zero. This minimises the responsivity of the interferometer intermirror distance to temperature fluctuations. Collected in Table 1 are the limiting relative instabilities of the mode frequency calculated for different materials and cavity lengths. One can see that the contribution from the cavity body is insignificant for almost all calculated configurations and that the stability is primarily determined by the thermal noise of the mirrors.

3. Lowering of the frequency instability limit caused by thermal noise

Among the ways of lowering the thermal noise, the following method should be mentioned : lowering the amplitude of the thermal noise itself and weakening the effect of thermal noise on the stability of cavity length.

The amplitude of thermal vibrations is determined by the specific amount of heat contained in a system and its dissipation power [13]. The amplitude may be lowered by lowering the operating cavity temperature and using high-Q mechanical materials – crystalline sapphire and silicon, fused silica, etc. – for making its components [10, 11, 16]. Also showing promise for this purpose is a change-over from the commonly employed high-reflectivity SiO_2/Ta_2O_5 coatings to the crystalline AlGaAs/GaAs ones, which possess a higher mechanical Q-factor [17].

One way to suppress the effect of thermal fluctuations on the cavity length is to increase the distance between the cavity mirrors. First, the relative frequency instability decreases with increasing length in accordance with formula (6). Second, in a longer cavity the TEM_{00} spot radius on the mirrors is longer and is defined by the expressions:

$$w_{01} = \left(\frac{\lambda}{\pi}\right)^{1/2}[L(R_1-L)]^{1/4}, \tag{7}$$

$$w_{02} = \left(\frac{\lambda}{\pi}\right)^{1/2}\frac{L^{1/4}R_1^{1/2}}{(R_1-L)^{1/4}}. \tag{8}$$

Formulas (7) and (8) apply to the mode of a Fabry–Perot cavity of length L consisting of a plane mirror and a concave spherical mirror with a radius of curvature R_1. In accordance with expression (3), increasing the mode spot on the mirror contributes to a higher stability of the value of $U_z(t)$ due to a greater area of thermal vibration averaging over the mirror surface.

Table 1. Limiting relative frequency instability of a cavity eigenmode induced by thermal noise.

Body/substrate/coating material	Cavity temperature/K	Cavity body length/mm	Relative frequency instability*	Body contribution (%)	Substrate contribution (%)	Coating contribution (%)
ULE glass/ULE glass/ (SiO_2/Ta_2O_5)	297	77.5	8.7×10^{-16}	0.5	65	34
ULE glass/fused silica/ (SiO_2/Ta_2O_5)	297	77.5	4.9×10^{-16}	2	1	97
ULE glass/fused silica/ (SiO_2/Ta_2O_5)	297	480	6.8×10^{-17}	11	1	88
Silicon/silicon/ (SiO_2/Ta_2O_5)	124	77.5	2.2×10^{-16}	10^{-3}	0.1	99.9

* The relative frequency instability caused by thermal noise may be lowered to 10^{-16} by using higher-Q materials, lowering the working temperature, and lengthening the cavity.

4. Finite element method for modelling suspension systems and determining the vibrational stability of long cavities

ULE glass, whose 'zero point' is close to the room temperature, is the traditional material for making high-Q cavities. The spectral linewidths of laser systems stabilised to ULE cavities approximately 10 cm in length range down to 0.5 Hz. A characteristic feature of ULE-glass cavities is an approximately linear frequency drift of about 0.1–1 Hz s^{-1} caused by material recrystallisation. The good linearity of the drift permits subtracting it and obtaining a relative instability of $\sim 10^{-15}$ on an averaging time frame of 1–10 s [18]. The thermal noise of short cavities becomes a hindrance to a further improvement of frequency stability. The 10^{-15} instability limit was overcome with the use of long monolithic cavities of mass ~20 kg with an intermirror distance of ~0.5 m [11, 19]. It is evident that lengthening a cavity heightens its sensitivity to vibrations as well as to fluctuations and uniformity of the temperature. Design and fabrication of long monolithic cavities is a challenging scientific and technical problem.

For the purposes of spectroscopy of the clock transition in a strontium optical clock, which now is under development at the VNIIFTRI [20], we designed two laser systems, in which 698-nm lasers are stabilised to 480-mm long external reference cavities of ULE glass in horizontal and vertical configurations. It is planned to make the mirror substrates of fused silica, which will permit the frequency instability limit induced by thermal noise to be lowered to 6.8×10^{-17} (see Table 1). The requirement of making two ultrastable systems is caused by the necessity of comparing their frequencies and determining the individual characteristics of each of the two systems [15]. The development of stabilisation systems with long ULE cavities brings up the burning question of temperature stability and vibrational cavity stability. Each configuration invites the design of a suspension system least sensitive to external vibrations.

The cavity length is affected by two types of mirror deformations under external forces: rotations and displacements (translations) [21]. A quantitative analysis of the elastic deformations of reference cavities performed by the method of finite elements [19] turns out to be highly beneficial when solving the optimisation problem, i.e. the search for supporting point positions whereby the displacements and tilts of cavity mirrors turn to zero simultaneously. Generally, to describe the vibrational susceptibility calls for a complete dynamic analysis of cavity motion under the action of periodic perturbing forces at different frequencies, but in our case we can restrict ourselves to the solution of the static problem for three reasons. First, of highest significance for our systems is low-frequency noise (with frequencies below 100 Hz), because it is poorly averaged over the short and medium times (1–100 s) of interest to us. Second, the higher frequency noise is quite well suppressed with the use of commercially available passive and active vibration isolation systems. Third, the wavelength of a sound wave in the cavity material is far greater than its geometric size. This signifies that different cavity parts oscillate in phase, and therefore it would suffice to consider the deformation induced by a constant 'instantaneous' force. It is noteworthy that the cavity eigenfrequencies usually exceed several kilohertz, which permits neglecting the resonance nature of vibrations in our consideration.

We denote the susceptibility to vibrations by $\boldsymbol{s}$ and define it in accordance with the expression

$$\frac{\Delta \hat{L}}{\hat{L}} = \boldsymbol{s}\boldsymbol{a}, \tag{9}$$

where $\boldsymbol{a}$ is the acceleration. We set ourselves the task of calculating the x-, y-, and z-components of vector $\boldsymbol{s}$. Also, the susceptibility pertaining to the mirror rotation will be denoted by $\boldsymbol{s}_t$ and the susceptibility pertaining to the mirror tilt by $\boldsymbol{s}_r$. In this case, $\boldsymbol{s} = \boldsymbol{s}_t + \boldsymbol{s}_r$.

Among the virtues of the horizontal cavity configuration is its low susceptibility to vertical perturbations when the supporting points are located at the so-called Airy points (Fig. 1a). Finding these points is a well-known problem in the theory of strength of materials: this is precisely how the bearings are located which support the length standard [22]. The possibility that there exists an arrangement such that the displacement and inclination angle of the mirrors turn to zero may be understood from the following reasoning. When the suspension points are close to each other, the cavity edges bend down under gravity and the mirror surfaces turn upwards. When the bearings are close to the edges, the central part of the interferometer body bends down and the mirrors turn downwards. Evidently there should be an intermediate arrangement of the bearing such that the mirror surfaces remain parallel to each

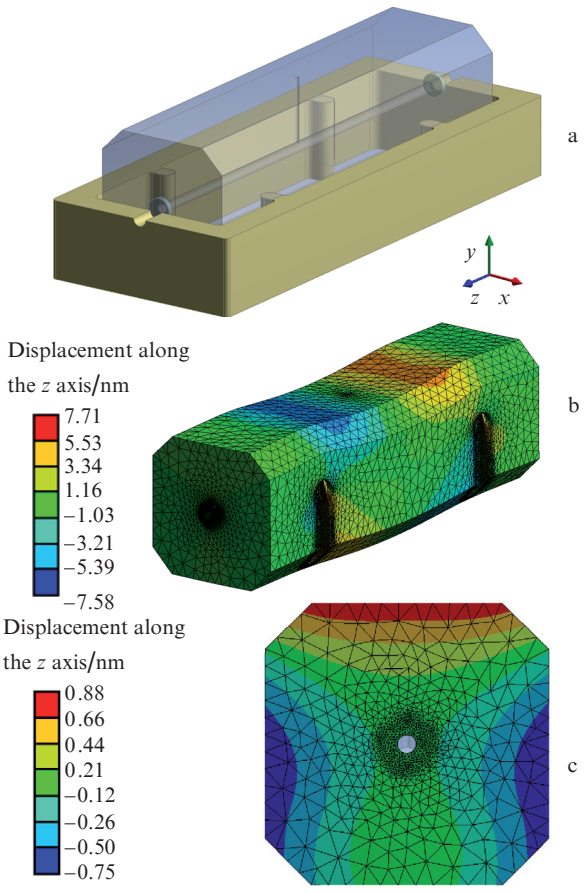

Figure 1. (Colour online) Model of vibration-immune suspension system for a horizontal ULE cavity: (a) the bearings are located at the Airy points, (b, c) deformations of a horizontal ULE cavity under the force of gravity.

other under the action of a vertical force. Similarly, when the upper face of the cavity is the plane of support, its body will stretch in the direction perpendicular to the optical axis, and the mirrors will come closer together due to the Poisson coefficient. When the lower face is the support plane, they will recede from each other. Therefore, a stable arrangement is always possible to find by optimising the depth d of position of bearings and their distance l from the cavity end face (Fig. 2a). Due to Hooke's law, the optimal arrangement is independent of the magnitude of the force that gives rise to elastic deformation.

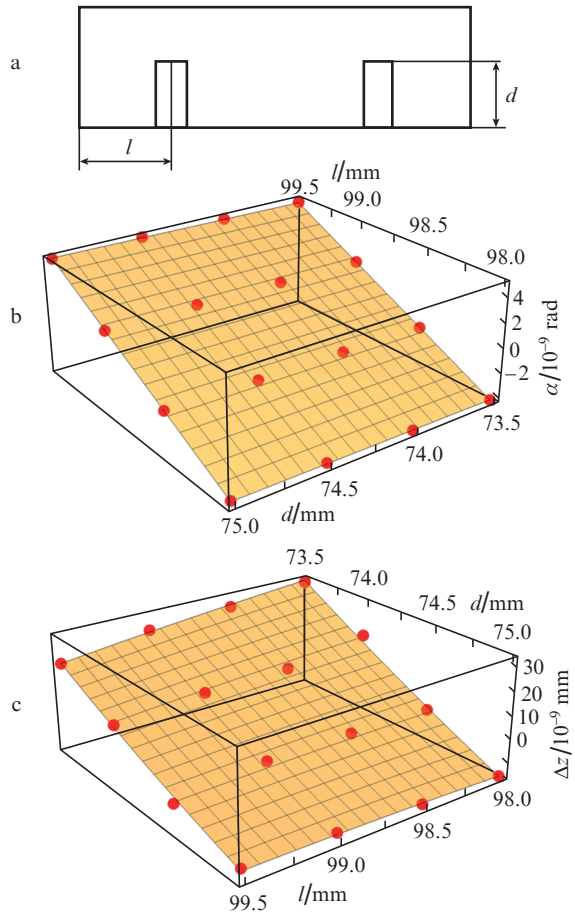

Figure 2. Parameters of cavity bearing points optimised in the course of finite-element simulations: (a) depth d of bearing location and their distance l from the cavity end face; (b, c) results of simulations: mirror tilt α and mirror displacement Δz on application of the force of gravity in relation to parameters d and l. Points and grey planes stand for the results of simulation and approximation.

The displacement and rotation of the cavity mirrors under the constant force of gravity was modelled by the method of finite-element analysis. Our simulations were made on a spatial grid consisting of $\sim 10^5$ tetrahedral and prismatic elements. The simulations were performed for different bearing parameters d and l. The calculated shifts and tilts are shown in Fig. 2b in relation to bearing coordinates.

Our simulations for a 480-mm long cavity of square section yielded the following optimal parameters of bearing positions: $l = 98.68$ mm, $d = 74.46$ mm. The gravity-induced cavity deformations with the use of the optimal parameters l and d are plotted in Figs 1b and 1c.

For a vertical arrangement of the cavity, it is fixed at three equidistant points located on its centre-of-mass plane (Fig. 3). This suspension system provides equal displacements of the upper and lower mirrors under the action of vertical forces and, accordingly, a high immunity to vibrations in this direction. Unlike the horizontal interferometer, the body of the vertical one is symmetrically cylindric in shape. The cavity body is 7 cm in diameter and 48 cm in length. The biconical shape of the interferometer body is most expedient as regards immunity to vibrations, because the greatest part of cavity mass is concentrated near the suspension points in this configuration (Fig. 3).

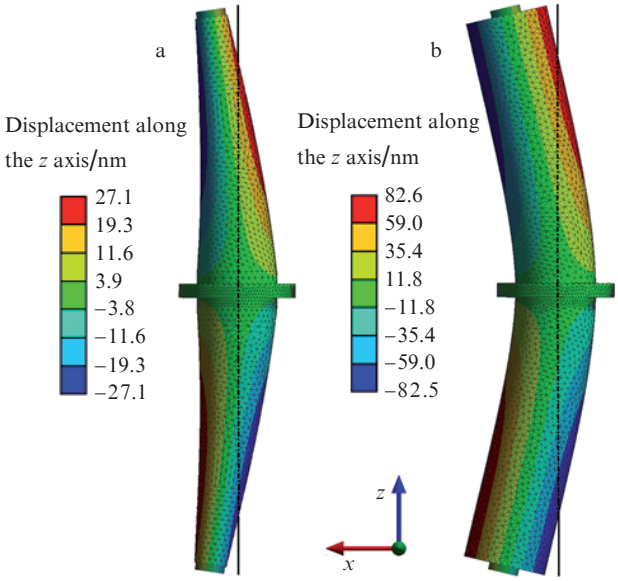

Figure 3. (Colour online) Deformations of (a) the vertical biconical and (b) cylindrical ULE cavities under the action of the same horizontal acceleration equal to 9.8 m s^{-2}. According to calculations, the use of biconical shape lowers the vibrational susceptibility by a factor of two.

We calculated the susceptibility to vibrations of the vertical and horizontal cavities for accelerations applied along different axes (Table 2). The susceptibility to all kinds of perturbations does not exceed $3 \times 10^{-10}/g$, with the exception of the susceptibility of the vertical cavity to horizontal accelerations. This characteristic should not become a factor that limits the cavity stability, because horizontal accelerations are normally several orders of magnitude weaker than the vertical ones in laboratory conditions.

5. Silicon cavity

Among the highly promising materials for high-Q optical cavities is monocrystalline silicon, which is transparent for the radiation with a wavelength ranging from 1.1 to 6.7 μm and has excellent mechanical characteristics. The fractional frequency instability of laser systems locked to silicon cavities has reached a presently record figure of 4×10^{-17} over an averaging time of 1–1000 s [10]. Furthermore, in silicon there are no ageing processes, which are responsible for the frequency drift in ULE cavities, which opens up the possibility of developing laser systems with a small (no greater than 2

Table 2. Susceptibility to vibrations of the vertical and horizontal ULE cavities of length 480 mm. Given are the contributions to the instability caused by mirror rotations (r) and translations (t) on application of accelerations along the x, y, and z axes (see Figs 1 and 3).

ULE cavity	Susceptibility to vibrations ($1/g$)					
	s_{rx}	s_{tx}	s_{ry}	s_{ty}	s_{rz}	s_{tz}
Vertical cylindrical	2×10^{-8}	2×10^{-8}	2×10^{-8}	2×10^{-8}	8×10^{-12}	1×10^{-10}
Horizontal	2×10^{-10}	1×10^{-10}	4×10^{-11}	4×10^{-11}	2×10^{-10}	3×10^{-10}

μHz s^{-1}) frequency drift [23]. With the use of a femtosecond generator of optical frequencies their stability may be imparted to any laser [24].

We pursue research aimed at developing laser systems that radiate at a wavelength of 1542 nm and are stabilised to silicon 7.75-cm long silicon cavities, whose thermal noise limit due to thermal noise is equal to 2.2×10^{-16} at a temperature of 124 K corresponding to the 'zero point' of silicon (Table 1). The use of a wavelength from the C band (near 1.5 μm) opens up the possibility of transmitting ultrastable signals via fibre lines over distances longer than 1000 km [25]. The cavity is cooled with the use of our developed cryogenic liquid-nitrogen system [26]. The cooler vessel is inside a vacuum chamber, and the heat exchange with the cavity is affected by thermal radiation. To maintain the level of cooler in the vessel, use is made of a system for the production and automatic transfer of liquid nitrogen. Its effect on cavity stability, which is produced by the vibrations emerging in the boiling of nitrogen, is eliminated by mechanically decoupling the vessel from the remaining part of the vacuum chamber. At a temperature of 124 K, the measured finesse F^* of the silicon cavity for the TEM_{00} mode was greater than 580000. The measurement was made by recording the ring-down of the light transmitted by the cavity (Fig. 4).

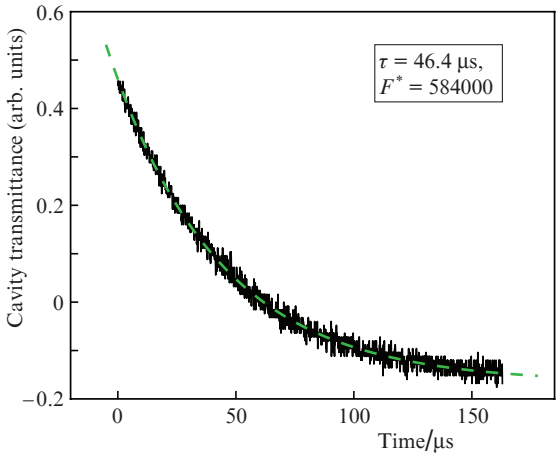

Figure 4. Measurement of cavity finesse F^* from the cavity transmittance decay time τ upon cutting off laser radiation: $F^* = 2\pi\tau c/(2L)$.

With the use of the silicon cavity we stabilised the output frequency of an erbium fibre laser at a wavelength of 1542 nm. The optical configuration of the facility was similar to that outlined in Ref. [18]. A slow feedback signal was delivered to a piezoelectric actuator and a fast feedback signal was applied to an acoustic modulator. This permitted obtaining a total loop bandwidth of about 100 kHz, which was limited by the PID controller in use. This bandwidth of the feedback loop was sufficient for stabilising the spectrally narrow (less than 10 kHz) emission of the fibre laser with a Bragg grating.

In the path to achieve the thermal noise limit, various electronic noise as well as the residual amplitude modulation of the laser radiation may be a serious problem. To realise the Pound–Drever–Hall technique, the laser radiation is phase-modulated by an electrooptical modulator (EOM). An inexact matching of the plane of light polarisation and the extraordinary axis of the EOM results in a parasitic amplitude modulation of the radiation. The modulation depth may vary due to temperature variation, which will introduce additional instability into the frequency stabilisation system. As shown in Ref. [27], the active compensation of amplitude modulation by applying feedback to the EOM permits its contribution to the radiation frequency instability to be diminished to a level defined by thermal noise and lower. We also plan to employ this technique in the future.

6. Conclusions

The research and development of ultrastable laser systems is among the key tasks in the development of optical frequency standards and optical frequency transmission lines as well as in the generation of radiofrequency fields with a high short-term stability in the problems of radio photonics. High-Q optical cavities make it possible to stabilise the output laser frequency to a residual relative instability of $\sim10^{-17}$, which is fundamentally limited by thermal noise. A series of investigations was carried out to develop laser systems stabilised to cavities with a low frequency instability limit imposed by thermal noise. To achieve a high frequency stability, advantage was taken of two approaches: the use of a long cavity and the application of new materials. For the cavity configurations under investigation and development, the fractional frequency instability corresponding to thermal noise was shown to be at a level of $\sim10^{-16}$. Cavity mount systems were investigated and optimised, and the attainable cavity susceptibilities to acceleration were shown to be equal to $\sim10^{-10}/g$. The systems under development will be employed in the optical frequency standard based on neutral strontium atoms at the VNIIFTRI for interrogating the clock transition at $\lambda =$ 698 nm and for stabilising the radiation frequency of a femtosecond optical frequency synthesiser.

Acknowledgements. This work was supported by the Russian Foundation for Basic Research (Grant No. 16-29-11723).

References

1. Kwee P., Bogan C., Danzmann K., et al. *Opt. Express*, **20** (10), 10617 (2012).
2. Chin C., Grimm R., Julienne P., Tiesinga E. *Rev. Mod. Phys.*, **82** (2), 1225 (2010).
3. Udem T., Reichert J., Holzwarth R., Hänsch T.W. *Opt. Lett.*, **24** (13), 881 (1999).

4. Bloom B.J., Nicholson T.L., Williams J.R., et al. *Nature*, **506** (7486), 71 (2014).
5. Chou C.W., Hume D.B., Koelemeij J.C.J., et al. *Phys. Rev. Lett*., **104**, 070802 (2010).
6. Quessada A., Kovacich R.P., Courtillot I., et al. *J. Opt. B: Quantum Semiclass*., **5** (2), 150 (2003).
7. Itano W.M., Bergquist J.C., et al. *Phys. Rev. A*, **47** (5), 3554 (1993).
8. Jiang Y.Y., Ludlow A.D., Lemke N.D., et al. *Nat. Photonics*, **5** (3), 158 (2011).
9. Drever R.W.P., Hall J.L., Kowalski F.V., et al. *Appl. Phys. B*, **31** (2), 97 (1973).
10. Matei D.G., Legero T., Häfner S., et al. *Phys. Rev. Lett*., **118** (26), 263202 (2017).
11. Häfner S., Falke S., Grebing C., et al. *Opt. Lett*., **40** (9), 2112 (2015).
12. Gillespie A., Raab F. *Phys. Rev. D*, **52** (2), 577 (1995).
13. Levin Yu. *Phys. Rev. D*, **57** (2), 659 (1998).
14. Numata K., Kemery A., Camp J. *Phys. Rev. Lett*., **93** (25), 250602 (2004).
15. Riehle F. *Frequency Standards. Basics and Applications* (Weinheim: Wiley, 2004; Moscow: Fizmatlit, 2009).
16. Storz R., Braxmaier C., Jäck K., et al. *Opt. Lett*., **23** (13), 1031 (1998).
17. Cole G.D., Zhang W., Martin M.J., et al. *Nat. Photonics*, **7** (8), 644 (2013).
18. Alnis J., Matveev A., Kolachevsky N., et al. *Phys. Rev. A*, **77** (5), 53809 (2008).
19. Martin M.J. Q*uantum Metrology and Many-Body Physics: Pushing the Frontier of the Optical Lattice Clock* (PhD dissertation, University of Colorado, 2013).
20. Berdasov O.I., Gribov A.Yu., Belotelov G.S., et al. *Quantum Electron*., **47** (5), 400 (2017) [*Kvantovaya Elektron*., **47** (5), 400 (2017)].
21. Millo J., Magalhães D.V., Mandache C., et al. *Phys. Rev. A*, **79** (5), 53829 (2009).
22. Phelps F.M. *Am. J. Phys*., **34** (5), 419 (1966).
23. Hagemann C., Grebing C., Lisdat C., et al. *Opt. Lett*., **39** (17), 5102 (2014).
24. Hagemann C., Grebing C., Kessler T., et al. *IEEE Trans. Instrum. Meas*., **62** (6), 1556 (2013).
25. Droste S., Udem T., Holzwarth R., Hänsch T.W. *Comptes Rendus Physique*, **16** (5), 524 (2015).
26. Zhadnov N.O., Masalov A.V., Sorokin V.N., et al. *Quantum Electron*., **47** (5), 1 (2017) [*Kvantovaya Elektron*., **47** (5), 1 (2017)].
27. Zhang W., Martin M.J., Benko C., et al. *Opt. Lett*., **39** (7), 1980 (2014).